INFLUENCE OF THE GEOMETRICAL NON-UNIFORMITY HOUSING SUPPORTS IN THE AUTOMOTIVE JOURNAL BEARINGS STRESSES DISTRIBUTION

Fernando de Azevedo Silva
Unesp – Faculdade de Engenharia de Guaratinguetá – Departamento de Mecânica
fazevedo@feg.unesp.br

Felipe José Passos Silva
Unesp – Faculdade de Engenharia de Guaratinguetá – Departamento de Mecânica
felipejpsilva@yahoo.com.br

Abstract. *This paper aim to use linear modeling, using finite elements method, in the analysis of the effect of geometrical non-uniformity in automotives journal bearings submitted to hydrodynamic stress distribution. For this, it will be used the commercial software ANSYS. Thus, it's intended to evaluate the relation between the stress distributions caused by geometrical non-uniformity with fatigue failure.*
The absence of support in part of the backing circumference can be consequence of the housing to present the following problems: manufacturing deficiency, rough surface finishing, insufficient squeeze of the screws, deformation caused by heating and brusque cooling. Solid impurities between bearing and housing also are considered non-uniformity causes.

Keywords: *Journal bearings, stress field, finite element method, geometrical non-uniformity.*

1. Introduction

The bearings for definition are elements that allow the relative movement between machines components, being their geometric form dependent of the relative movement nature that it desires to get. In the case of the journal bearing, two surfaces slide one over other and support radial forces that tend to bring the two surfaces in contact in a limit situation.

The performance of the bearings in all conditions of operation has been the target of several scientific studies. Many factors can cause the bearing failure. These are related to the design and sizing, the manufacture and the operational conditions.

The analysis of stresses distribution in service become prerequisite in the development of studies applied to prediction bearing failures (Hacifazlioglu, 1996; Wilcock, 1957).

There are many stress sources in bearings, as, for example, pressure gradient, flexibilities of backing and housing materials, presence of oil grooves, non-uniform housing supports and temperature distributions, surface roughness, backing layer thickness, covering layer thickness, assembly problems, among others.

In this paper had been carried out static structural analyses in an automotive bearing of current use in an industry, through finite elements, using commercial program ANSYS, version 7.0, to verify the effect of geometrical non-conformity in automotives journal bearings submitted to hydrodynamic stress distribution. Thus, it's intended to connect the stress distribution with fatigue failure.

The absence of support in part of the backing circumference can be consequence of the housing to present the following problems: manufacturing deficiency, rough surface finishing, insufficient squeeze of the screws, deformation caused by heating and brusque cooling. Solid impurities between bearing and housing also are considered non-conformity causes.

In accordance with Norton (1998), the active hydrodynamic pressure in the bearing can be gotten from Ocvirk solution for short bearings, as shown to follow (DuBois, 1955):

$$p = \frac{\eta U}{r c_r^{\,2}} \left[\frac{l^2}{4} - z^2 \right] \frac{3\varepsilon \operatorname{sen}\theta}{(1+\varepsilon\cos\theta)^3} \tag{1}$$

where:

η: Absolute viscosity [mPa.s];
U: Linear velocity [m/s];
r: Journal radius [m];
c_r: Radial clearance [m];

l: Journal length [m];
z: Escape direction (it is considered null for short bearings);
ε: Excentricity ratio; and
θ: Pressure angle [rad].

2. Definition of the bearing discrete model

In the analysis, the bearing models were developed in the bidimensional plan, inside of the elastic regime and it was assumed that deformation along the bearing longitudinal axis (coordinate axis *z*) doesn't occur. This situation characterizes the plain state of deformation. Basing on the article published for Ibrahim and McCallion (1970), the adopted simplification is a realistic consideration to the usual relations of length and diameter of the radials slide bearings.

The bearings developed to the analysis are constituted by a fine wall backing of steel recovered with an antifriction alloy of *babbitt* tin base. In all implemented models a perfect adhesion in the interface between covering material and backing of steel was considered. This situation allows admitting displacements continuity in the interface region.

The used dimensions for the bearing standard geometry definition were gotten of an automotive bearing (figure 1) in use currently for an industry assembly plant.

Figure 1. Photo of the automotive journal bearing in study.

Table 1 presents the main dimensions that served of base for the construction of the bearing geometrical model. This standard model possesses completely rigid housing and it was used as reference in results comparison.

Table 1. Main dimensions used in the geometries construction.

Component	**Outer Diameter** [*D*]	**Inner Diameter** [*d*]	**Thickness** [*e*]	**Length** [*l*]
Backing	44.00 mm	41.58 mm	1.21 mm	18.01 mm
Covering	41.58 mm	41.08 mm	0.25 mm	18.01 mm

Table 2 presents the necessary mechanical properties for the implementation of the bearing finite elements models.

Table 2. Necessary mechanical properties for the models development.

Componente	**Material**	**Modulus of Elasticity**	**Poisson Coefficient**
Backing	Steel carbon	207 GPa	0.292
Covering	*Babbitt* tin base	50 GPa	0.330

The bearing geometrical model was developed from two concentrical rings, being that this ring was parted in four circulars arcs that are guided in accordance with the boundary conditions (displacements restrictions) and loading.

With the definition of the geometrical model it was proceeded the discrete finite elements model generation. For this, in all models, bidimensional, quadrilateral and isoparametric with eight nodes solid elements were used.

The baking of steel and the *babbitt* covering layer becomes discretes using the *PLANE 82* element through a mapped mesh of 120 x 6 and 120 x 4 finite elements, respectly. Figure 2 presents in detail the finite elements mesh gotten, being able to notice the elements distribution for each layer (backing and covering).

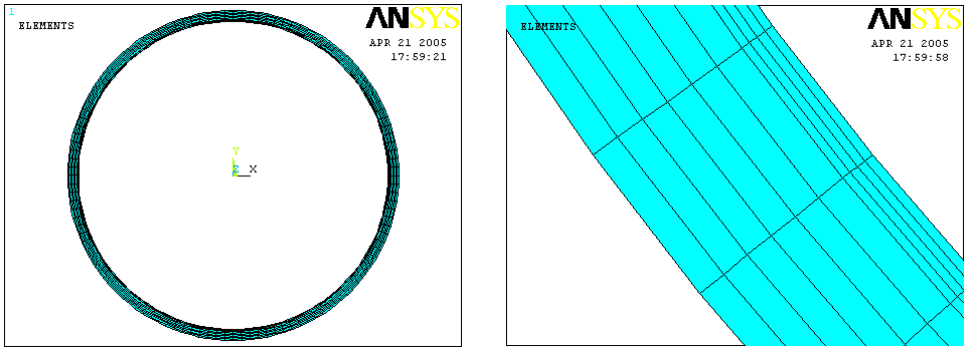

(a) (b)

Figure 2. (a) Mapped mesh of *PLANE82* elements; (b) Highlight to the layer of 6 elements in the baking of steel region and of the 4 elements in the *babbitt* covering layer.

3. Application of the boundary conditions

The possible radial displacements in the bearing were impeded along of all external circumferences for the standard model. Already for the implemented models to simulate the condition where there is loss of support supplied by housing to the bearing (geometrical non-conformity), the restriction was partial.

Also was impeded the circumferential displacement to the value of the pressure angle θ equal π. This displacement restriction simulates the rebound found in the bearings to fix them in the connecting rod housing.

The least procedure before solution is to define and to apply the hydrodynamic pressure distribution load of the oil film on the bearing. This also is a most laborious procedure, because it is necessary the previous knowledge of the polynomial function that represents the oil pressure to be applied in the ANSYS.

Figure 3 presents the bearing discrete model with the application of the constraints to the possible displacements, corresponding a bearing with perfectly rigid housing and totally supported in the housing, as also, shows the schematical representation in the ANSYS of the loading applied in the bearing.

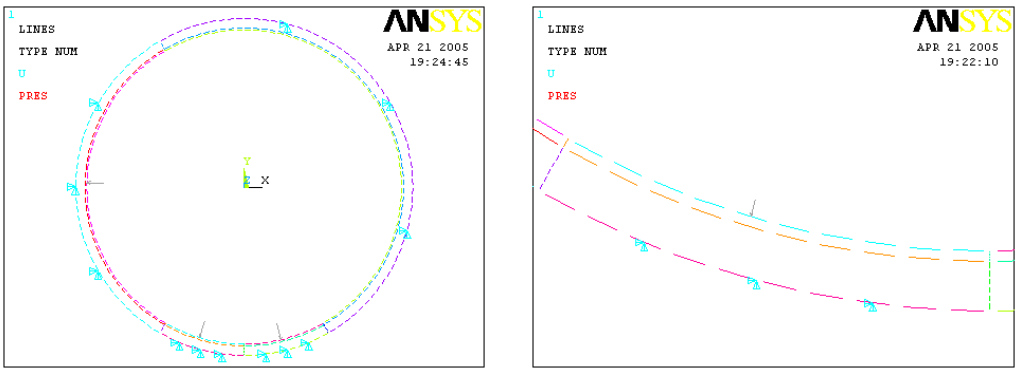

(a) (b)

Figure 3. (a) Bearing discrete model showing displacements constraints (triangles) and applied pressure on the *babbitt* surface (arrows); (b) Detail of this displacements constraints and applied pressure.

4. Stresses analysis in the bearing

The active circumferential stresses in the bearing are presents in the figure 4. Although they are almost totally of compressive nature, the circumferential stresses starts to be tensile in the pressure angle θ equal 300^{o}, in the other words, in the end of the region that hydrodynamics pressure acts and in the neighborhood where the biggest pressure gradients occurs.

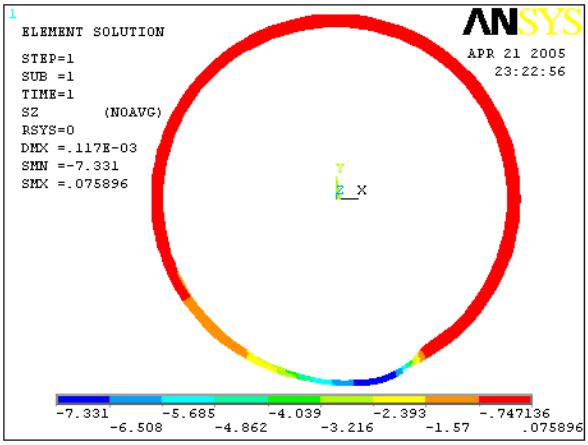

Figura 4. Circumferential stresses to the model with perfectly rigid housing.

The circumferential stresses distribution in the bearing surface is present in the figure 5a. To the model with complete and perfectly rigid housing, the circumferential stress is compressive nature in the region under hydrodynamic pressure. Its bigger intensity, in module, occurs in the maximum pressure point. The contour of active shear stresses in the backing/covering interface is presented in the figure 5b.

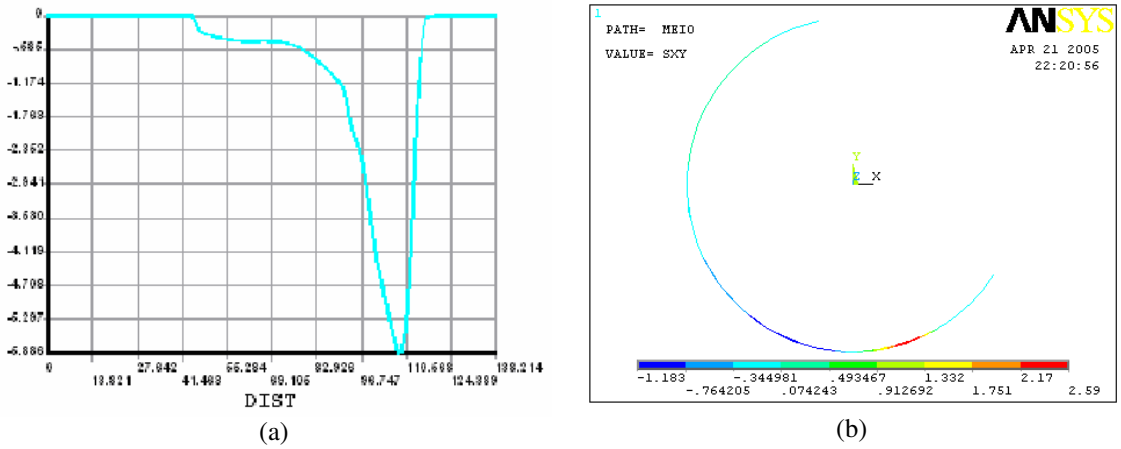

(a) (b)

Figure 5. (a) Circumferential stresses distribution in the bearing surface; (b) Contour of shear stresses in the backing/covering interface.

5. Influence of the housing non-uniformity

The absence of the connecting rod housing support (sustentation) in part of the backing of steel circumference can be caused by a series of reasons, among which: manufacture process faulty, rude finishing of the housing surface, insufficient squeeze of the housing screws (connecting rod cover), housing deformation caused by heating and brusque cooling, and the presence of strange solid particles between the bearing backing and the housing (Hacifazlioglu, 1996).

Usually, this situation impedes the adjusted contact between bearing and connecting rod housing, causing bend distortions in the covering surface and making it difficult the heat flow.

In this paper two conditions of housing support absence were simulated in part of the bearing, in other words, partial support to $120° \leq \theta \leq 300°$ (bearing section that hydrodynamics pressure acts) and partial support to $300° \leq \theta \leq 480°$ (bearing section with absence of pressure), where expects that it causes the most adverse effect.

5.1. Condition of conformity between bearing and housing ($120^o \leq \theta \leq 300^o$)

Figure 6 presents the influence of the geometrical non-conformity between bearing and housing on the circumferential stresses in the bearing with incomplete support.

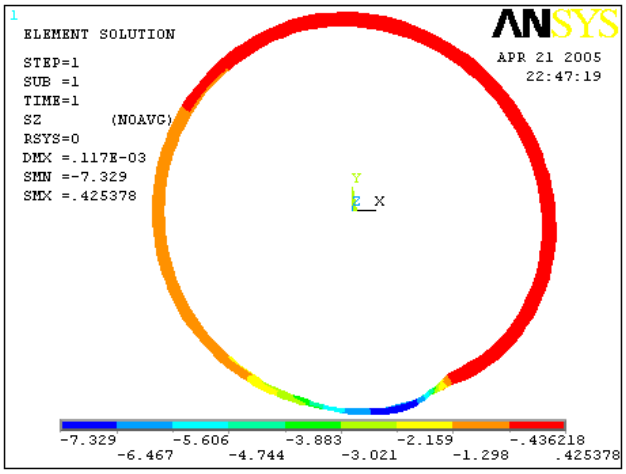

Figure 6. Circumferential stresses in the bearing with incomplete support.

Figure 7 shows the circumferential stresses distribution that acts in the bearing surface with partial support in the pressure region.

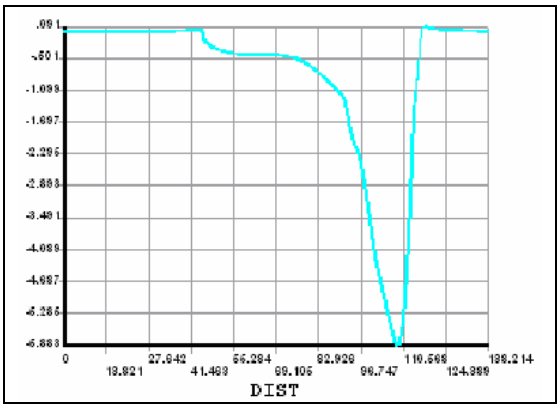

Figura 7. Circumferential stresses distribution in the surface.

The influence of the geometrical non-conformity between bearing and housing on the shear stresses in the backing/covering interface can be observed in the figure 8.

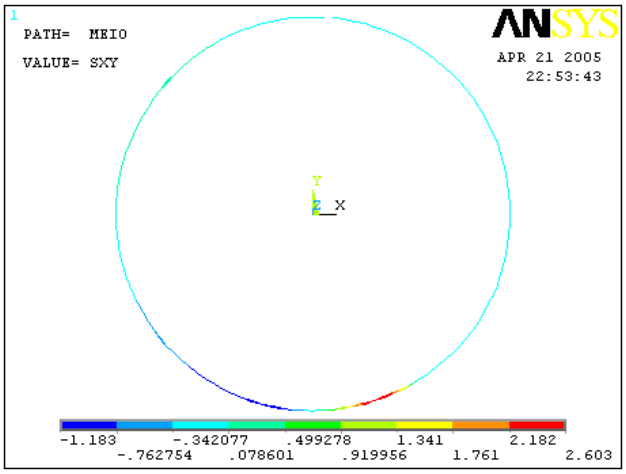

Figure 8. Shear stresses in the backing/covering interface.

The shear stresses distribution in the interface between backing and covering is presented in the figure 9.

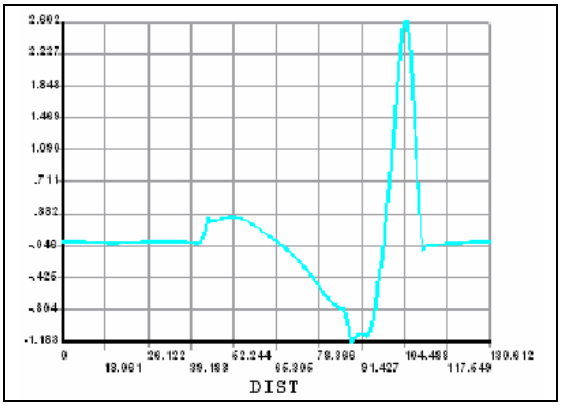

Figure 9. Shear stresses distribution in the backing/covering interface.

It is verified that the bearing with incomplete support only in the pressure region is less affected by non-conformity between bearing and housing, as much to the circumferential stresses, as to the shear stresses in the interface between backing and covering.

5.2. Condition of conformity between bearing and housing ($300^o \leq \theta \leq 480^o$)

Figure 10 presents the bearing displacement profile resultant of the hydrodynamic pressure action and of the absence of support in the pressure region. In this figure, it can observe that the bearing has its form modified in the regions where finish the housing support. In these regions occur located strains that can results in high stresses.

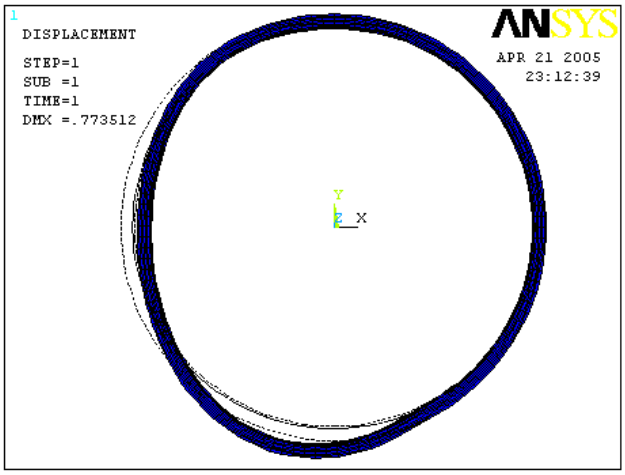

Figure 10. Displacement profile to the bearing with the support in the without pressure region.

Figure 11 presents the circumferential stresses in the bearing. Analyses with support absence in the neighborhood of the maximum pressure region indicate that these stresses can achieve values greater to the resistance limit of the covering material.

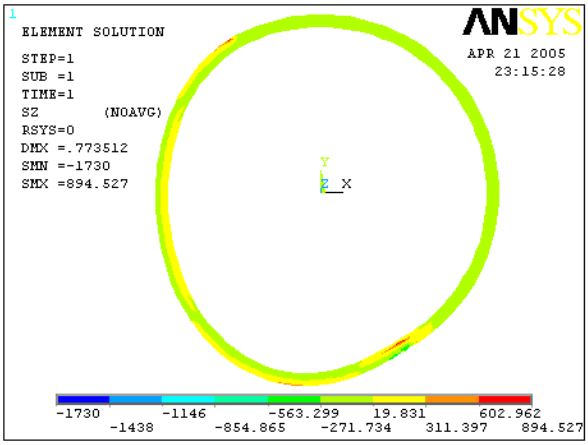

Figure 11. Circumferential stresses to the partial support in the region without pressure.

In the figure 12 it can be observed the influence of the incomplete support proportionate by housing to the bearing limited to the region that where the pressure don't acts, in the circumferential stresses that acts in the bearing surface.

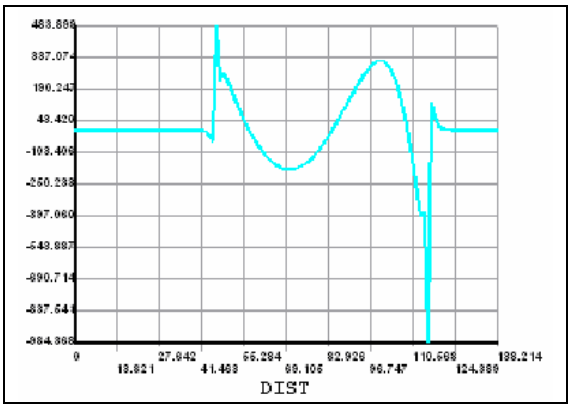

Figure 12. Circumferential stresses distribution in the bearing surface.

An analysis of the values presented in the figures 11 and 12 allows to observe that the support absence in the pressure region in the bearing favors the fatigue failure, due to the increase of the tensile circumferential stresses intensity originated from the bend distortion that occur in the end of the pressure region.

An analysis of the figure 13 allows verifying that the housing non-conformity has strong influence on the shear stresses in the backing/covering interface to the incomplete support conditions only in the region without pressure.

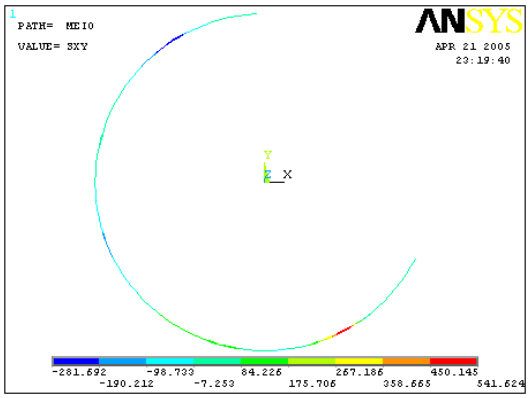

Figure 13. Shear stresses in the backing/covering interface.

In the same way as it occurs with the circumferential stresses in the bearing surface, an alteration is observed in the distribution and in the intensity of the shear stresses in the regions under pressure where there is loss of support.

In the table 3 are presented the maximum values in module of the gotten stresses in function of the three simulated conditions of geometrical conformity between bearing and housing.

Table 3. Maximum circumferential and shear stresses to the different supports.

Stress field	Total support	Partial support ($120^o \leq \theta \leq 300^o$)	Partial support ($300^o \leq \theta \leq 480^o$)
Circumferential	7.331 MPa	7.329 MPa	1730.0 MPa
Circumferential in the surface	5.886 MPa	5.884 MPa	984.368 MPa
Shear	3.126 MPa	3.271 MPa	1076.0 MPa
Shear in the interface	2.590 MPa	2.603 MPa	541.624 MPa

Comparing the model with complete support to the model with partial support in pressure region, it is observed that the maximum circumferential stresses practically remain unchanged, with exception of the shear stresses that presents a small gain.

The value of the maximum shear stress that occurs in the interface between backing and covering is 2.59 MPa to the model with total support. It is noticed that this value starts to be so bigger, 541.62 MPa, to the model with partial support only in the region without pressure.

In the case of partial support only in the region without pressure occurs a significative increase of the all stresses intensity, when compared to the reference model.

6. Conclusions

- The adopted condition of the housing to be considered perfectly rigid is a rather simplified hypothesis. In the reality doesn't exist any perfectly rigid structure, but how the analysis had limited a cylindrical ring of steel (backing) covered by antifriction alloy and not to the study of housing deformation, the adopted procedure is in accordance with the published paper scientific community (Hacifazlioglu, 1996; Ibrahim, 1970; Thomazi, 2000).
- Assuming that doesn't have none another influence on the bearing surface, as also, that no surface possesses excellent finishing, is considered that fatigue cracks propagates from surface micro-cracks that function as stresses concentration, mainly in regions where the major tensile stresses acts.
- It is observed that the circumferential and shear stresses are influenced by geometrical non-uniformity condition, mainly when the housing support absence in part of the backing circumference occurs in the hydrodynamic pressure region.
- In the analysis of the circumferential stresses in the bearing surface and of the shear stresses in the interface between backing of steel an covering of *babbitt* is possible to identify stresses concentration regions, where occurs support absence. These can facilitate the nucleation of fatigue cracks process.

7. References

DuBois, G. B., Ocvirk, F. W., Ithaca, N. Y., *The Short Bearing Approximation for Plain Journal Bearings*, Transactions of the ASME, pp. 1173-1178, 1955.

Hacifazlioglu, S., Karadeniz, S., *A Parametric Study of Stress Sources in Journal Bearings*, Int. J. Mech. Sci., vol. 38, nº 8-9, pp. 1001-1015, 1996.

Ibrahim, S. M., McCallion, H., *Stresses in Oil Lubricated Bearings*, vol. 184, nº 3, pp. 69 – 78, Proc. Inst. Mech. Engrs., 1970.

Norton, R. L., *Machine Design: An Integrated Approach*, Prentice-Hall Inc., 1998.

Thomazi, C. C., Pérez, M. M., Oliveira, S. A. G., *Influência da Não-conformidade Geométrica entre Alojamento e Mancal sobre o Campo de Tensões de Bronzinas*, Anais em CD do CONEM 2000, Congresso Nacional de Engenharia Mecânica, Natal, RN, 2000.

Wilcock, D. F., Booser, E. R., *Bearing Design and Application*, 1ª ed., McGraw-Hill Book Company, Inc., 1957.

8. Responsibility notice

The authors are the only responsible for the printed material included in this paper.